ORIGINAL ARTICLE

Annual dynamics of *Zymoseptoria tritici* populations in wheat cultivar mixtures: A compromise between the efficacy and durability of a recently broken-down resistance gene?

Carolina Orellana-Torrejon[1,2] | Tiphaine Vidal[1] | Anne-Lise Boixel[1] |
Sandrine Gélisse[1] | Sébastien Saint-Jean[2] | Frédéric Suffert[1]

[1]Université Paris-Saclay, INRAE, AgroParisTech, UMR BIOGER, Thiverval-Grignon, France

[2]Université Paris-Saclay, INRAE, AgroParisTech, UMR ECOSYS, Thiverval-Grignon, France

Correspondence
Frédéric Suffert, Université Paris-Saclay, INRAE, AgroParisTech, UMR BIOGER, 78850 Thiverval-Grignon, France.
Email: frederic.suffert@inrae.fr

Funding information
Fond de Soutien à l'Obtention Végétale; French Ministry of Education and Research; Saclay Plant Sciences-SPS, Grant/Award Number: ANR-17-EUR-0007

Abstract

Cultivar mixtures slow polycyclic epidemics but may also affect the evolution of pathogen populations by diversifying the selection pressures exerted by their plant hosts at field scale. We compared the dynamics of natural populations of the fungal pathogen *Zymoseptoria tritici* in pure stands and in three binary mixtures of wheat cultivars (one susceptible cultivar and one cultivar carrying the recently broken-down *Stb16q* gene) over two annual field epidemics. We combined analyses of population "size" based on disease severity, and of population "composition" based on changes in the frequency of virulence against *Stb16q* in seedling assays with more than 3000 strains. Disease reductions were observed in mixtures late in the epidemic, at the whole-canopy scale and on both cultivars, suggesting the existence of a reciprocal protective effect. The three cultivar proportions in the mixtures (0.25, 0.5, and 0.75) modulated the decrease in (a) the size of the pathogen population relative to the two pure stands, (b) the size of the virulent subpopulation, and (c) the frequency of virulence relative to the pure stand of the cultivar carrying *Stb16q*. Our findings suggest that optimal proportions may differ slightly between the three indicators considered. We argue potential trade-offs that should be taken into account when deploying a resistance gene in cultivar mixtures: between the dual objectives "efficacy" and "durability," and between the "size" and "frequency" of the virulent subpopulation. Based on current knowledge, it remains unclear whether virulent subpopulation size or frequency has the largest influence on interepidemic virulence transmission.

KEYWORDS
cultivar mixture, resistance breakdown, *Stb16q*, virulence, wheat disease epidemics, *Zymoseptoria tritici*

1 | INTRODUCTION

The industrialization of agrosystems has greatly simplified the implementation of crop protection. In conventional cereal farming, fungal disease control is based on two major pillars: phytosanitary products and disease-tolerant or resistant cultivars. Most fields are planted with a single cultivar, in which effective resistance usually depends on the combination of a few qualitative resistance genes

rather than diversified quantitative genetic components. The strong resistance conferred by a single gene is simpler for breeders to handle, but may be easily overcome by pathogens (McDonald & Linde, 2002).

The number of wheat cultivars grown in north-western Europe is small (Perronne et al., 2017). This leads to the exertion of unidirectional selection pressures on plant pathogen populations, fostering the breakdown of qualitative resistances, and resulting in an increase in the frequency of virulent strains just after their emergence (Brown & Tellier, 2011). Host homogeneity thus limits the durability of qualitative resistance, defined as its efficacy over a prolonged period of widespread use under conditions conducive to the disease (Johnson, 1984). Pathogen evolution, which occurs at a variable rate, usually results in the replacement of the oldest cultivars grown with others carrying new sources of resistance. These dynamics have been widely described in publications on wheat diseases as a response to the common boom-and-bust cycles observed in clonal pathogen populations (e.g., McIntosh & Brown, 1997) and to the more gradual breakdown of resistance in diversified sexual populations (e.g., Cowger et al., 2000). In this context, one of the most striking issues currently facing us is the need to reconcile the efficacy and durability of the resistances available to farmers, by identifying optimal strategies for their deployment over different space-time scales (Fabre et al., 2015).

Increasing crop diversity at the field scale has been widely reported to result in more effective control over plant disease epidemics. This is the case for cultivar mixtures (Wolfe, 1985), in which cultivars of the same species with complementary traits, including those relating to plant immunity, are grown together. Cultivar mixtures have long been considered particularly effective against airborne fungal pathogens (Borg et al., 2018; Cowger & Mundt, 2002a) and were widely used at the end of the last century in some European countries. The use of wheat mixtures has increased in Europe in recent years, reflecting a growing interest in their beneficial effects. In France, for instance, the percentage of the national area occupied by mixtures of bread wheat cultivars has doubled over the last four years (4.8% in 2017, 8.6% in 2018, 11.9% in 2019, and 12.2% in 2020; FranceAgriMer, https://www.franceagrimer.fr). The factors affecting the efficacy of cultivar mixtures against splash-dispersed diseases, such as Septoria tritici blotch (STB) on bread wheat, have also been investigated, with a combination of experimental and modelling approaches (Gigot et al., 2013; Kristoffersen et al., 2019; Vidal et al., 2017). The proportions of susceptible and resistant cultivars in the mixture are known to have a determinant effect on disease reduction (Borg et al., 2018; Finckh et al., 2000; Gigot et al., 2014). Nevertheless, most of the experimental approaches focused on the impact of mixtures on the overall canopy, with the aim of using the most resistant plants to protect the susceptible plants, and little is known about the consequences for the most resistant cultivar. The value of cultivar mixtures for controlling diseases lies in the complementarity of the cultivar phenotypes, providing a guarantee of efficacy. However, cultivar mixtures may affect the evolution of pathogen populations, by diversifying the selection pressures exerted by their plant hosts at field scale, potentially with different effects on the different cultivars in the mixture. Little is known about pathogen evolution (changes in virulence gene frequencies) in cultivar mixtures, particularly during the early stages of resistance gene breakdown, that is, when the frequency of virulent strains remains low.

The heterothallic ascomycete fungus *Zymoseptoria tritici*, which causes STB, is responsible for yield losses averaging 20% on susceptible bread wheat cultivars in north-western Europe (Fones & Gurr, 2015). The development of epidemics is dependent on both splash-dispersed asexual pycnidiospores during the wheat growing period and wind-dispersed ascospores from sexual reproduction on crop residues (Figure 1a; Suffert et al., 2011). The potential intra-annual selective dynamics and strong genetic recombination within *Z. tritici* populations make STB a good candidate model for investigating the issues described above. Cultivars carrying qualitative and quantitative resistances have been developed and used to control STB, leading to an overall increase in the mean resistance of commercial wheat cultivars registered in France in the last decade (from 5.2 in 2015 to 6.0 in 2019, on a scale of 1 to 9, with 9 corresponding to the most resistant cultivar; ARVALIS-Institut du Végétal/CTPS). In total, 21 *Stb* genes and 89 quantitative trait loci (QTLs) have been identified and mapped (Brown et al., 2015). *Stb16q*, one of the most recent major resistance genes to have been incorporated into several cultivars by breeders, initially provided high levels of resistance against STB in both seedlings and adult plants (Ghaffary et al., 2012). *Stb16q* is present in 13 wheat cultivars registered in France between 2012 and 2018, including cv. Cellule (Florimond Desprez, France). Cellule was widely used in France, becoming the third most frequent cultivar grown (8% of the area under wheat in 2016), but its use then declined following a decrease in its resistance to STB. Indeed, STB symptoms were first observed on Cellule in 2015 in France (Romain Valade, ARVALIS-Institut du Végétal, personal communication) and in 2019 in Ireland (Kildea et al., 2020), highlighting the beginning of a breakdown of *Stb16q* resistance.

In this epidemiological study, our goal was to investigate the capacity of mixtures to reduce disease, as a short-term epidemiological outcome, and to interfere with the resistance breakdown process, as an evolutionary outcome. In field experiments, we analysed the effect of the proportion of wheat plants carrying the qualitative resistance gene *Stb16q* within a binary wheat mixture on the size (disease severity) and composition (frequency of virulent strains) of *Z. tritici* pathogen populations during an annual epidemic.

2 | MATERIALS AND METHODS

2.1 | Overall strategy

We compared the two-year dynamics of natural *Z. tritici* populations in pure stands and in binary mixtures of wheat cultivars, from the early to late stages of a field epidemic (Figure 1a). We combined analyses of population "size" based on disease severity in the field as
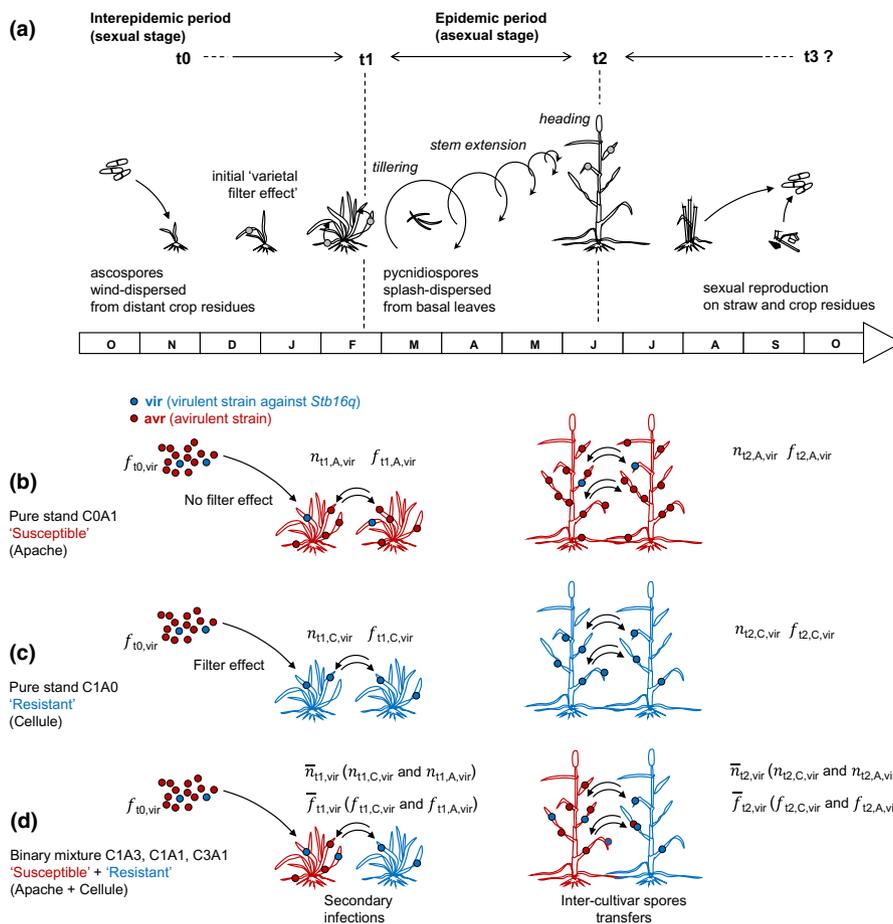
FIGURE 1 (a) Overview of the development of a Septoria tritici blotch epidemic adapted to (b, c) two pure stands and to (d) a mixture of the two wheat cultivars, one carrying the *Stb16q* resistance gene, and the other lacking this gene (cv. Cellule in proportion p_C and cv. Apache in proportion $1-p_C$). The size of the pathogen population can be expressed as $n_{t,v,vir}$ (size of the virulent subpopulation on the cultivar $v \in [A; C]$ at time $t \in [t1; t2]$) and $\bar{n}_{t,vir}$ (size of the virulent subpopulation on the whole canopy at time t). The composition of the pathogen population is expressed as $f_{t,v,vir}$ (frequency of virulent strains on cultivar v at t) and $\bar{f}_{t,vir}$ (frequency of virulent strains on the whole canopy at time t), with $f_{t0,vir}$ the initial frequency of virulent strains in the local pathogen population

a proxy, and of population "composition" based on estimations of the proportion of virulence against *Stb16q* obtained by screening several thousands of field-collected strains in seedling assays. To this end we developed and applied an in planta "population phenotyping" strategy in a greenhouse. We then reinforced this strategy by confirmatory individual phenotyping in more suitable climatic conditions in a growth chamber rather than in a greenhouse (Table S3), to increase the reliability of characterization for some of the strains.

2.2 | Cultivars studied

This study focused on two bread wheat (*Triticum aestivum*) cultivars: Apache ('A'; Limagrain, France) was chosen for its moderate susceptibility to STB (rated 4.5, stable over time, on a scale of 1 to 9, where 9 corresponds to the most resistant cultivar, ARVALIS-Institut du Végétal/CTPS), and Cellule ('C'; Florimond Desprez, France), which carries the *Stb16q* resistance gene (rated 7 in 2016 vs. 5 in 2020,

ARVALIS-Institut du Végétal/CTPS). Apache was the predominant cultivar in France from 2000 to 2010, accounting for 24% of the area under wheat in 2003, subsequently falling to less than 5% after 2015 (Figure 2a). Cellule, registered in 2012, became the third most frequently used French cultivar, but the area under this cultivar rapidly decreased after 2016 (Figure 2b). Both cultivars were well represented in the Parisian basin and, thus, probably played a significant role in the evolutionary trajectory of the local pathogen populations collected in 2018 and 2019.

2.3 | Design of the field experiment

We carried out a field experiment at the INRAE experimental station at Thiverval-Grignon (France) in the 2017/2018 and 2018/2019 seasons. A field plot was divided into three blocks (a, b, and c), each consisting of five microplots (3.5 m wide × 8 m long, with an inter-row spacing of 0.175 m; Figures S1 and S2). These microplots
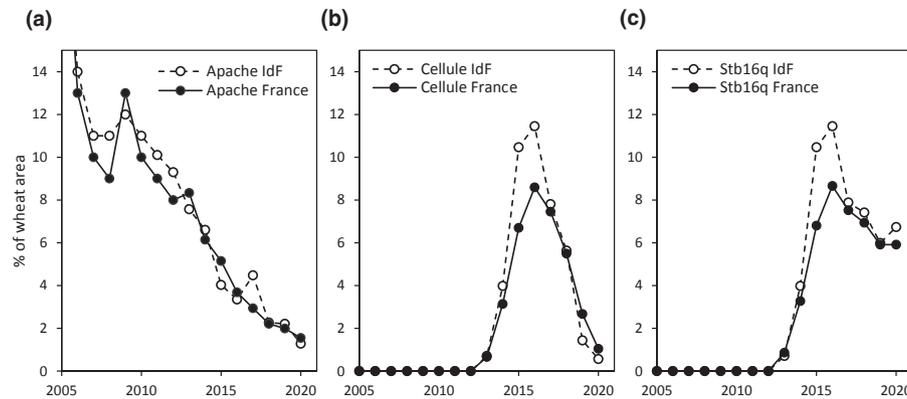
FIGURE 2 Changes in the percentage of the area under wheat sown with (a) cv. Apache, (b) cv. Cellule, and (c) the 13 cultivars carrying *Stb16q* in France (black dots) and in the Parisian basin (Région Ile-de-France "IdF"; white dots) from 2005 to 2020 (FranceAgriMer data sets)

corresponded to five randomly distributed treatments: a pure stand of wheat cv. Apache (C0A1; Figure 1b), a pure stand of wheat cv. Cellule (C1A0; Figure 1c), and three binary mixtures, with sowing proportions of Cellule (p_C) of 0.25, 0.5, and 0.75 (C1A3, C1A1, and C3A1; Figure 1d). The wheat was sown on 17 October 2017 and 15 November 2018, at a density of 220 seeds/m^2. The seeds were treated with the insecticide tefluthrin at a dose of 0.2 g/kg (Attack; Syngenta France SAS) to minimize early attacks of aphids, known to transmit yellow dwarf viruses, especially barley yellow dwarf virus (BYDV). The seed lots were prepared by considering the specific weight of seeds for each cultivar (thousand-kernel-weight) to obtain the proportions of seeds required for each treatment. The sowing was performed using the different seed lots leading to a "random cultivar mixture" at the microplot scale. Differentiation between the two cultivars—a key point of the experiment—was adapted to each growth stage: (a) at seedling stage, the identification was made according to a dye included in the seed coating (red for Cellule, green for Apache; Figure S2b); (b) later in the season, the identification was made according to the bearded (Cellule) or unbearded (Apache) nature of the inflorescence (Figure S2e). We estimated the actual proportions of each cultivar late in the growing season, at heading, by counting spikes of each cultivar along three 1-m lines in each microplot (Figure S1, Table S1). Nitrogen fertilizer applications were adjusted by the balance-sheet method with a target yield of 7 t/ha. A single herbicide treatment was applied in the early spring. No fungicide treatment was applied.

2.4 | Characterization of the pathogen population size

We used disease severity (i.e., diseased leaf area) as a proxy for the size of the pathogen population (i.e., the number of asexual offspring), assuming the two traits to be correlated (Suffert et al., 2013). Disease severity was measured at leaf scale as the percentage of leaf area covered by pycnidia (sporulating or not). For the sake of simplicity, this measure is hereafter called "sporulating area". Sporulating area was scored as 0, 1%, 3%, 5%, 10% and then increments of 5%

up to 100%. It was assessed visually early in the epidemic (time t1; Zadoks stage 15), before the expression of most of the secondary infections, and then late in the epidemic (time t2; Zadoks stage 70), just after the disease had reached the upper leaves (Figure S2). The t1 assessments of disease severity were performed on various dates (from 5 to 12 March in 2018 and 27 February to 18 March in 2019), due to experimental constraints. We collected 10 seedlings of each cultivar from each microplot, on which disease severity was scored for the five lowest leaves. At t2, similar disease severity assessments were performed for the five upper leaves (L1 to L5 from the top to the bottom of the plant) of 10 plants of each cultivar per microplot, on 11 May 2018 and 18 June 2019. The optimal scoring window varies with epidemic dynamic. Scoring was therefore performed earlier in 2018 (intense early epidemic) than in 2019 (moderately intense late epidemic). The flag leaves (L1) were assessed a second time, in all microplots, on 15 June 2018 and 26 June 2019. The complete data set is presented in supplementary files F1–3.

A disease severity index (SEV) was calculated at the plant scale. At t1, SEV was calculated as the mean sporulating area over all non-senescent leaves. At t2, SEV was calculated as the mean sporulating area of representative leaf layers (L4 and L3 in 2018, and L3 and L2 in 2019), excluding those with a mean severity below 1% or completely senescent on more than two microplots.

A mean disease severity index (SEV_v) was then calculated for each cultivar *v* for each treatment. An overall mean disease severity index ($\overline{SEV}$) was also calculated at the whole-canopy scale for each treatment, using SEV_v weighted by the proportions of the cultivars (p_C for Cellule and $1 - p_C$ for Apache), as follows:

$$\overline{SEV} = p_C \times SEV_C + (1 - p_C) \times SEV_A \qquad (1)$$

We assessed the effect of treatment on the disease severity index SEV at t1 and t2, and analysed changes in this effect over the course of each epidemic. To this end, SEV was transformed by ordered quantile normalization (*bestNormalize* R package). Its variance was partitioned into sources attributable to the following factors and their interactions: cultivars (A; C), treatments (C0A1; C1A3; C1A1; C3A1; C1A0), blocks (a; b; c), epidemic stages (t1; t2), and

years (2018; 2019), according to the generalized linear model. The model was adjusted by removing non-significant interactions one-by-one. For SEV_v and $\overline{SEV}$, standard errors were corrected by taking into account the error propagation of formulas.

The effect of treatment on SEV_A and SEV_C at each stage of each year was first assessed with a Tukey HSD post hoc test for multiple pairwise comparisons on estimated marginal means (*emmeans* and *multcomp* R packages). The variance of the overall disease severity index $\overline{SEV}$ was then estimated by calculating the standard error. The effect of cultivar mixtures on $\overline{SEV}$ was evaluated by plotting the expected $\overline{SEV}$ (assuming an absence of mixture effect) as a linear function of the severity in each pure stand weighted by Cellule proportions. All data analyses were performed with R software (v. 4.0.2 R Core Team 2012).

2.5 | Characterization of the pathogen population composition

2.5.1 | Sampling of strains in the field

Strains of *Z. tritici* were collected at t1 and t2 in 2018 and 2019, to constitute groups of 30 strains per cultivar and per microplot (total of 3060 strains; Table 1 and supplementary file F4). The sampling effort was doubled in the pure stands of the susceptible cultivar at t1 in 2018 and 2019 (2 × 180 strains). The population present on cv. Apache early in the epidemic (t1), which may be considered a representative sample of the primary inoculum population, was used to estimate the initial (t0) frequency of virulent strains ($f_{t0\text{vir}}$; Figure 1b).

We ensured that 30 strains were obtained per cultivar from each microplot by sampling 40 lowest leaves of seedlings at t1 and 40 flag leaves of adult plants at t2. These samples were placed in a humid chamber to promote the extrusion of cirrhi. One cirrhus per leaf was picked with a pin and streaked onto a Petri dish containing potato dextrose agar (PDA; 39 g/L), which was then incubated at 18°C for more than 5 days in the dark. A few blastospores from a single colony were then picked and spread on a new plate. This operation was repeated twice to obtain pure single-spore strains.

Each strain was finally scraped off the plate, to obtain a substantial mass of blastopores (150 mg), which was deposited at the bottom of cryotubes and stored at −80°C. At t1 in 2018, we sometimes had to collect more than one strain per leaf to counterbalance the low level of severity on certain microplots or the degradation/senescence of the diseased leaves. In both situations, we picked cirrhi from two to three distinct, distant lesions present on the same leaf.

2.5.2 | Phenotyping strategy

We characterized the *Z. tritici* strains for virulence (defined by Niks et al., 2011 as "the capacity of a pathogen to infect a plant with one or more major genes for resistance") against *Stb16q* and their aggressiveness (the quantitative term of pathogenicity on a susceptible host; Lannou, 2012). We developed a population phenotyping method for use on cv. Cellule and cv. Apache seedlings in the greenhouse (Figure S3), which allowed us to individually characterize a large number of strains while accepting some imprecisions or individual errors quantified a posteriori. This approach was complemented by confirmatory individual phenotyping in growth chambers, in which we characterized several dozens of strains that were collected from sporulating lesions on Cellule in the field but appeared avirulent during population phenotyping. This made it possible to determine the rate of type II error (false avirulence) for population phenotyping.

2.5.3 | Population phenotyping

Population phenotyping was performed from April 2018 to August 2020, by splitting the 3060 strains into 32 batches of 102 (t1) or 93 (t2) strains, which were simultaneously tested in the greenhouse (Figure 3). Each batch was balanced to contain similar numbers of strains from each cultivar, treatment, and block. Eight virulent strains were added to each batch as control strains. Wheat seeds (cv. Apache or Cellule) were sown in 0.4-L pots, to obtain three 18-day-old seedlings per pot. The pots were kept in the greenhouse

TABLE 1 Number of *Zymoseptoria tritici* strains sampled on each cultivar for each treatment (C0A1, C1A3, C1A1, C3A1, and C1A0), at the early (t1) and late (t2) stages of the 2018 and 2019 epidemics, and phenotyped to determine virulence status

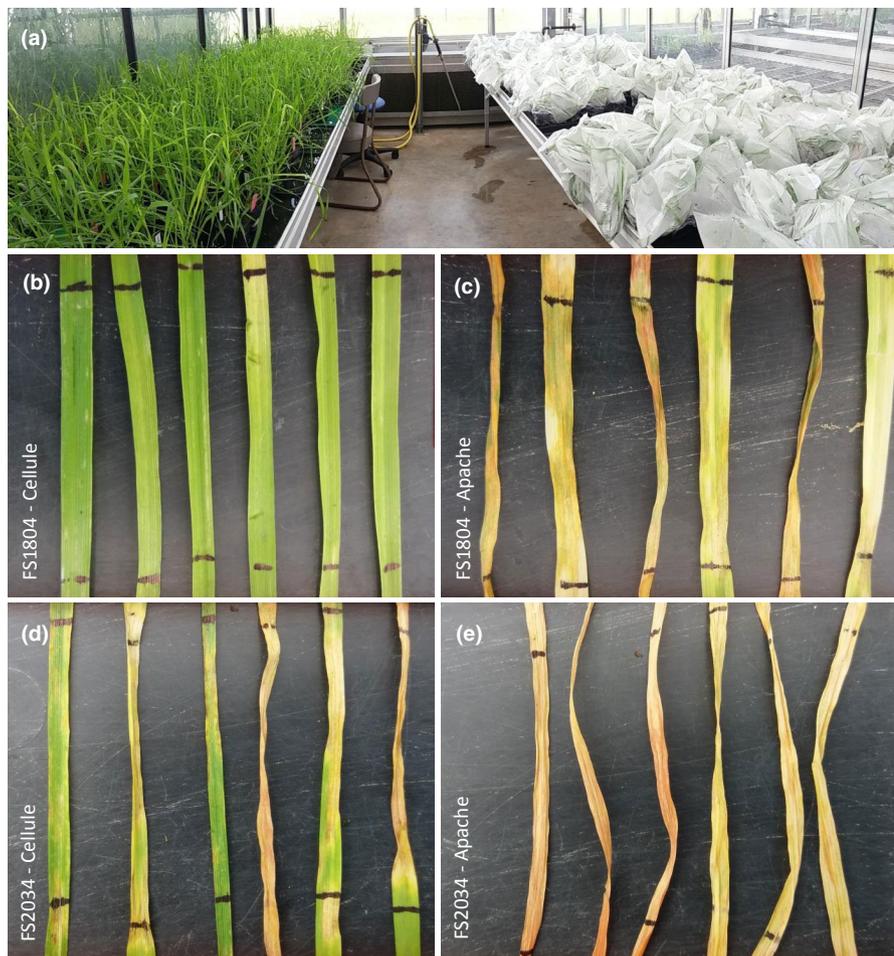| Year | Stage | C0A1 | C1A3 | | C1A1 | | C3A1 | | C1A0 | |
		A	C	A	C	A	C	A	C	Total
2018	t1[a]	179	90	90	90	90	90	87	90	806
	t2[b]	90	90	90	89	90	90	90	90	719
2019	t1[c]	180	82	88	88	84	90	89	90	791
	t2[d]	90	90	90	90	90	90	89	90	719

Note: Cultivars: A, Apache; C; Cellule.
[a]Collected from 5 to 12 March.
[b]Collected from 13 June.
[c]Collected from 27 February to 13 March.
[d]Collected from 25 June.

FIGURE 3 (a) Example of two 102-strain batches, one obtained just after inoculation (right) and the other one week later (left). (b–e) Typical incompatible–compatible interaction between the FS1804 (avirulent against *Stb16q*) and FS2034 (virulent against *Stb16q*) strains on six Cellule and Apache leaves (for each interaction, three second leaves on the left and three third leaves on the right)

under natural daylight supplemented with 400 W sodium vapour lamps to homogenize the lighting conditions. The temperature was kept below 20°C during the 15-h light period and above 15°C during the 9-h dark period. Relative humidity was kept at a mean value of 68 ± 9%. The thermal time at which disease severity was assessed was calculated for each batch (Figure S5).

We simplified the classical method based on accurate adjustment of a blastospore suspension, by considering that the differences in disease severity induced by the differences in concentration within the range 10^5 to 5×10^5 spores/ml (see Figure 8 in Suffert et al., 2018) were acceptable for our objective. We thus used unadjusted suspensions in this range of concentrations. For each strain, we diluted in 30 ml of water the blastospores recovered directly with a 10 µl inoculating loop (about 10 mg in the half-filled central ring; Sarstedt) from the freshly thawed content of the cryotube preserved at −80°C . Two series of independent tests showed that this process provided a good compromise between robustness and repeatability (Figure S4). Two drops of surfactant (0.1% vol/vol Tween 20; Sigma) were added to each suspension, to increase its adhesion to leaves. All suspensions were prepared the day before inoculation and stored at 5°C. A cotton bud was used to inoculate a 5 cm midlength leaf section by two back-and-forth passages over the second and third leaves from the bottom on seedlings previously described. This way, each strain was tested individually on two leaves of the

three seedlings of the pot (six replicates), for each cultivar. Each pot was then enclosed in a sealed transparent polyethylene bag moistened with distilled water for 72 h, to promote infection.

Disease severity was assessed visually 21 days postinoculation (dpi; mean thermal time 434.8°C·days for the 32 batches; Figure S5), as the percentage of the inoculated leaf surface covered by pycnidia (sporulating area assessed, from 0 to 100%, in increments of 5%). The complete data set is presented in supplementary file F5. A strain was considered virulent ('vir') against *Stb16q* when pycnidia were observed on at least one of the six leaves of Cellule (at least 5% of sporulating area on the leaf, the minimum for visual quantification in our experimental conditions). The strains were otherwise considered avirulent ('avr'). The frequency of virulent strains $f_{t,v,vir}$ ($t \in$ [t1; t2], $v \in$ [A; C]) was calculated for each cultivar in each treatment (Figure 1b–d). The effect of the treatment on the number of virulent individuals was assessed with a χ^2 test, or with Fisher's exact test when the expected numbers were small, with Bonferroni correction for pairwise comparison. We analysed the changes in $f_{t,v,vir}$ from t1 to t2, assessing the year effect with a test of equal or given proportions (*stats* R package). The initial frequency of virulent strains in the local pathogen population ($f_{t0,vir}$; Figure 1b–d) in 2018 and 2019 was estimated by characterizing the 180 strains from the pure stand of cv. Apache. We postulated that in this treatment the initial "filter effect" exerted on a strain according to its virulence

status with respect to *Stb16q* was negligible ($f_{t1,A,vir} = f_{t0,vir}$ in C0A1; Figure 1b).

We calculated the aggressiveness (AG) and conditional aggressiveness (AGc), defined as the amount of disease "conditional on the individuals being infected" (McRoberts et al., 2003). AG was estimated as the mean sporulating area on all leaves of the susceptible cultivar, whereas AGc was calculated only on leaves with symptoms, to take into account the absence of symptoms on some leaves (due to the less suitable climatic conditions in the greenhouse than in the growth chamber; Table S3). For a given strain, AGc was thus calculated under the condition that at least three of the six inoculated leaves presented pycnidia. Furthermore, we assessed the possible fitness cost of virulence against *Stb16q*, by evaluating the effect of virulence on aggressiveness. Because of the non-normality of data and the shape of the distribution curve, we used a generalized linear model adapted to a Poisson distribution, followed by a Tukey HSD post hoc comparison (*car* R package). The variance of each aggressiveness trait (AG and AGc) was partitioned into sources attributable to the following factors and their interactions, in pairs: the virulence status of the strain (vir; avr), treatment (C0A1; C1A3; C1A1; C3A1; C1A0), the cultivar of origin (A; C), year (2018; 2019), epidemic stage (t1; t2), block (a; b; c), and batch (1–32).

2.5.4 | Confirmatory individual phenotyping

A second round of phenotyping was applied to 47 strains that did not fulfil the requirement to be considered virulent against *Stb16q* during the population phenotyping in the greenhouse, despite having been isolated from sporulating lesions on Cellule in 2018 (see the Results section). For this purpose, we used Cellule (C) and two isogenic lines of the wheat cultivar Chinese Spring without *Stb6* (naturally present in Chinese Spring; Chartrain et al., 2005), one of which carried *Stb16q* (CS-*Stb16q*) whereas the other did not (CS). The strains were split into three batches and tested individually in a growth chamber (Figure S3). A virulent and an avirulent strain were added to each batch as controls. Inoculum suspensions were adjusted to a density of 5×10^5 spores/ml with a Malassez cell. Leaves were inoculated by applying the suspension with a paintbrush, on the second leaf from the bottom of nine seedlings of each cultivar. The temperature in the growth chamber was kept below 20°C during the 15-h light period and above 15°C during the 9-h dark period. Relative humidity was maintained at a mean of 88.5 ± 1.2%. Disease severity was assessed visually 14, 20, and 26 dpi, as the percentage sporulating area. The virulent, avirulent, or nonpathogenic nature of each strain was determined by calculating the mean aggressiveness (mean percentage of sporulating area on a leaf obtained across the nine replicates) and comparing it to a classical 10% of sporulating area threshold (Thierry Marcel, INRAE BIOGER, personal communication) rather than 5% in the greenhouse (less suitable climatic conditions; Table S3). A strain was considered (a) virulent against *Stb16q* if the mean aggressiveness was equal or higher than this threshold on both CS-*Stb16q* and Cellule, (b) avirulent if it was equal or higher than this threshold on

CS only, or (c) nonpathogenic if it was below this threshold on the three cultivars (Figure S10). The mean aggressiveness of strains was compared between CS-*Stb16q* and Cellule with a Wilcoxon test. The effect of treatment on the number of avirulent strains was assessed with Fisher's exact test.

2.6 | Overall impact of cultivar mixtures on the dynamics of virulent subpopulations

We calculated the percentage of the diseased leaf area occupied by virulent strains at t2 ($n_{t2,v,vir}$; $v \in$ [A; C]; Figure 1b–d), as a proxy for the size of the virulent subpopulations responsible for the last asexual disease cycle. This dimensionless variable was obtained by multiplying the disease severity index (SEV_v) on the flag leaves of each cultivar in each microplot by the frequency of virulent strains estimated at t2 ($f_{t2,v,vir}$). The mean size of the virulent subpopulations ($\overline{n}_{t2,vir}$) and the mean frequency of virulent strains ($\overline{f}_{t2,vir}$) were calculated at the whole-canopy scale for each treatment (Figure 1b–d), as for overall disease severity index ($\overline{SEV}$, Equation 1). The effect of treatment on $n_{t2,v,vir}$ and $\overline{n}_{t2,vir}$ was assessed in a Kruskal–Wallis test.

3 | RESULTS

3.1 | Impact of cultivar mixtures on the dynamics of the epidemic and the overall size of pathogen populations

Disease was generally less severe in the mixtures than in the two pure stands late in the epidemic, when the whole canopy was considered, and on both cultivars relative to their pure stands. This can be interpreted as a reciprocal protective effect.

At t1 in 2018, no significant difference in mean disease severity index (SEV_v) was observed between pure stands and mixtures, regardless of the cultivar considered, except for Apache in C1A1 ($p = 0.987$, $p = 0.042$, and $p = 0.155$ for Apache and $p = 0.172$, $p = 0.388$, and $p = 0.065$ for Cellule in C1A3, C1A1, and C3A1, respectively; Figure 4). In mixtures, Apache was on average 1.6 times more attacked than Cellule, consistent with their resistance ratings. The modelling results showed that the variance of disease severity index (SEV) was not attributable to the block factor ($p = 0.090$). Overall disease severity index $\overline{SEV}$ decreased with the proportion of Cellule.

At t1 in 2019, SEV_A and SEV_C were lower than in 2018. In mixtures, Apache was on average 2.8 times more attacked than Cellule. In pure stands, SEV_A scored 17% and SEV_C scored 4% (data not shown). $\overline{SEV}$ decreased with the proportion of Cellule.

At t2 in 2018, SEV_v differed significantly between pure stands and mixtures for Cellule, but not for Apache ($p = 0.397$, $p = 0.148$, and $p = 0.357$ for Apache and $p < 0.001$, $p < 0.001$, and $p = 0.089$ for Cellule in C1A3, C1A1, and C3A1, respectively; Figure 4). In pure stands, Apache was on average 1.5 times more attacked than
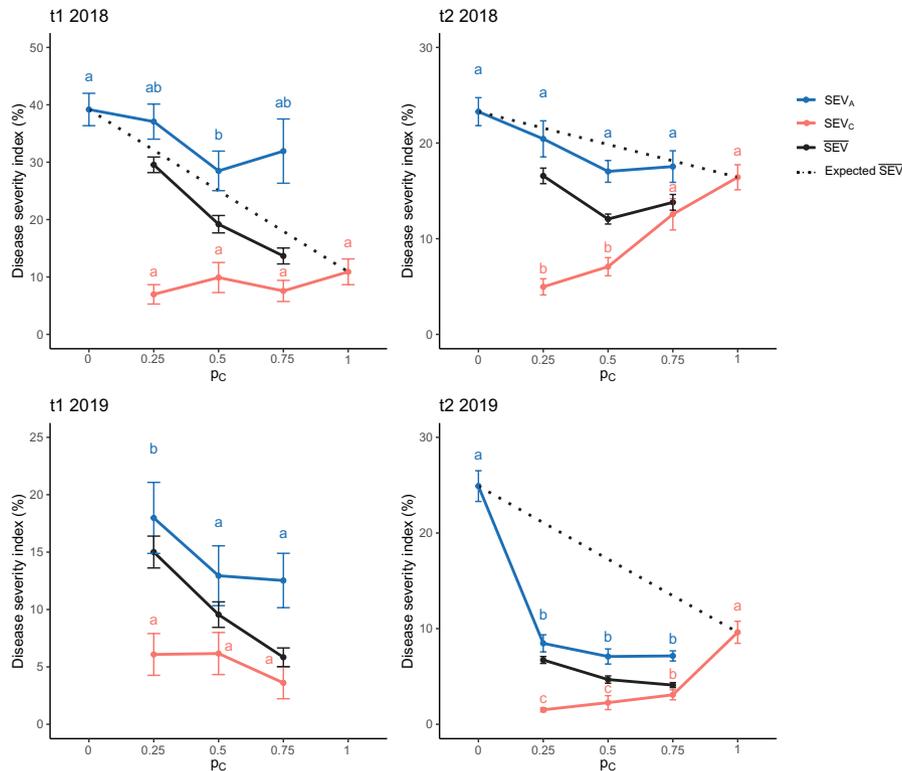
FIGURE 4 Mean disease severity index SEV_v (mean percentage of the leaf area covered by pycnidia on cultivar v) according to the proportion of cv. Cellule (p_C) in the canopy. SEV_A (blue solid line) and SEV_C (red solid line) were calculated from disease assessments in the field. Bars represent the standard error. Significant differences in SEV_A and SEV_C between p_C are indicated by letters (generalized linear model followed by a Tukey HSD post hoc test). The overall severity index $\overline{SEV}$ (black solid line) was calculated at the whole-canopy scale as the mean of SEV_A and SEV_C weighted by the proportion of each cultivar. The expected $\overline{SEV}$ (in the absence of a mixture effect) was plotted as a linear function of the severity in each pure stand weighted by p_C (black dotted lines). SEV_A, SEV_C, and the expected $\overline{SEV}$ in pure stands at t1 in 2019 are not shown because disease severity was assessed one week earlier than in mixtures

Cellule. In mixtures, SEV_A was on average reduced by 20% and SEV_C, to a greater extent, reduced by 48% compared to the respective pure stands. At the whole-canopy scale, $\overline{SEV}$ was lower in the three mixtures than in pure stands.

At t2 in 2019, SEV_v differed significantly between pure stands and mixtures for both cultivars, this difference being more significant than in 2018 ($p < 0.0001$ for Apache and $p < 0.0001$ for Cellule in all C1A3, C1A1, and C3A1). In pure stands, Apache was 2.5 times more attacked than Cellule. In mixtures, SEV_A was on average reduced by 69% and SEV_C reduced by 73% compared to the respective pure stands. The decreases in SEV_A, SEV_C, and $\overline{SEV}$ in mixtures relative to pure stands was more pronounced in 2019 than in 2018.

The overall effect of treatment was illustrated by plotting the expected $\overline{SEV}$ as a linear function of the severity in each pure stand weighted by Cellule proportions (p_C; Figure 4), which accounts only for "dilution" in mixtures. The actual and expected $\overline{SEV}$ curves were close at t1 in 2018 whereas the actual $\overline{SEV}$ was below the expected $\overline{SEV}$ at t2 for the two years considered. This highlights the overall absence of a mixture effect on disease dynamics at t1, at least in 2018, and the strong mixture effect at t2 for both years. The efficacy of the various treatments relative to pure stands was 19%,

40%, 22% in 2018 and 67%, 71%, 69% in 2019, for C1A3, C1A1, and C3A1, respectively.

3.2 | Impact of mixtures on the composition of pathogen populations

In total, 3035 of the 3060 *Z. tritici* strains sampled during the two years were characterized for virulence and aggressiveness, by inoculating 36,420 leaves of wheat seedlings in the greenhouse. The cultivar mixtures increased the frequency of virulent strains from the early (t1) to late (t2) stages in the two epidemic years.

The frequency of virulence at t1 ($f_{t1,A,vir}$) was estimated on Apache in pure stands at 0.13 in 2018 and 0.14 in 2019 (Figure 5). These frequencies are not significantly different (χ^2 test, $p = 0.791$), and the two years may therefore be considered as "replicates". The frequency of virulent strains on Apache did not differ significantly between treatments at t1, confirming the absence of a mixture effect early in the epidemic. The frequency of virulent strains on Apache at t2 ($f_{t2,A,vir}$) in pure stands was 0.08 in 2018 and 0.18 in 2019, and was not significantly lower than that at t1 (test of equal

FIGURE 5 Frequency of *Zymoseptoria tritici* strains considered virulent (grey bars) against *Stb16q* (i.e., causing sporulating area on cv. Cellule) and avirulent (white bars) among the populations collected on cv. Apache in pure stands ($p_C = 0$) and mixtures ($p_C = 0.25$, 0.5, and 0.75 for C1A3, C1A1, and C3A1, respectively) at the early (t1) and late (t2) stages of the 2018 and 2019 epidemics. The number of virulent and avirulent strains are indicated in grey and white boxes, respectively. The effect of treatment (pure stands and cultivar mixtures; letters at the top of each bar) on the number of virulent strains was assessed by performing a χ^2 test with Bonferroni correction for pairwise comparison
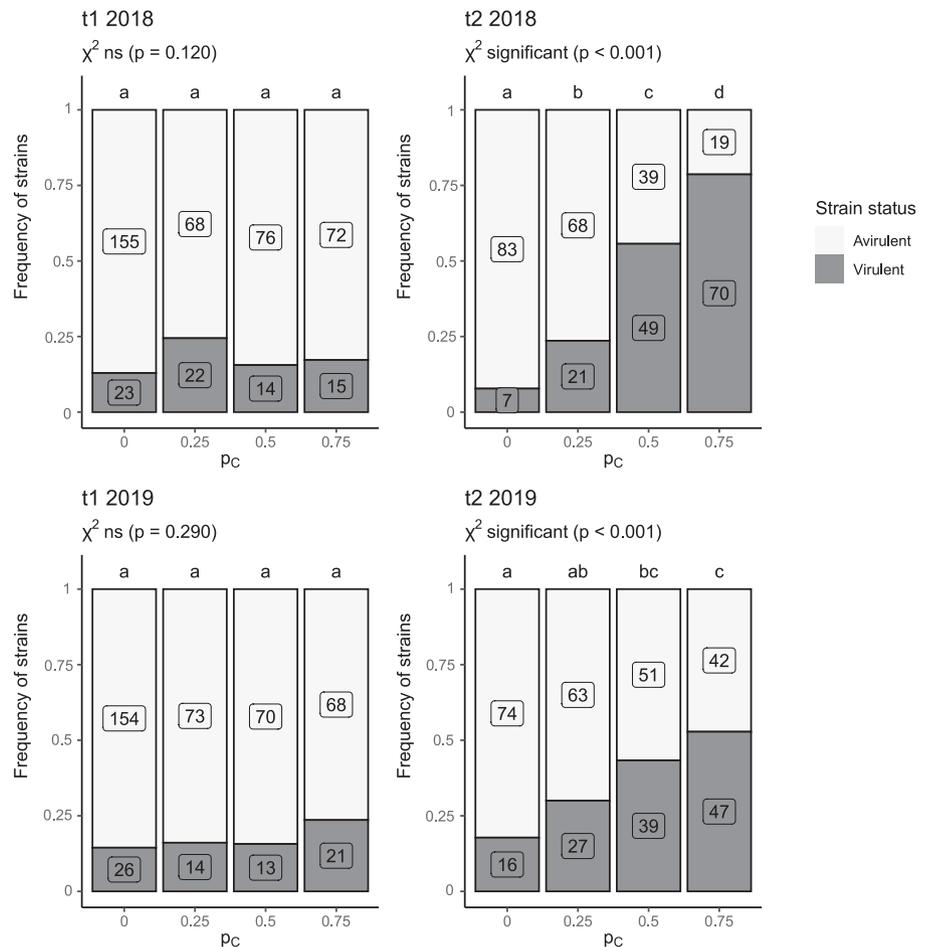
or given proportions, $p = 0.244$). Importantly, in mixtures, $f_{t2,A,vir}$ increased significantly with p_C both years.

Very few strains were classified as nonpathogenic: 0.3% (5/1525) in 2018 and 0.1% (2/1510) in 2019 (Figures S6 and S7). Most of the strains (>95%) induced pycnidia on Apache, with no significant difference between treatments. The percentage of strains that did not induce pycnidia on Apache was low: 4% (31/719) and 3% (23/710) for those collected on Cellule in 2018 and 2019, respectively, and 6% (50/806) and 5% (38/800) for those collected on Apache in 2018 and 2019, respectively. Strains collected on Cellule were expected to be virulent, as a consequence of the "filter effect" exerted by *Stb16q* (Figure 1c). However, 7% of these strains (52/719) in 2018 and 10% (74/710) in 2019 (Figure 6) did not induce pycnidia on Cellule during phenotyping. The proportion of these strains, considered avirulent after population phenotyping, did not differ significantly between treatments. Only 2% of the strains (27/1525 in 2018 and 20/1510 in 2019, distributed across all treatments) induced pycnidia on Cellule but not on Apache.

Confirmatory individual phenotyping showed that 51% (24/47) of the strains tested for a second time were avirulent, 34% (16/47) were virulent, and the results were dubious for 15% (7/47). The overall percentage of "truly avirulent" strains collected on Cellule in 2018 was thus estimated at a maximum of 3% (24/719). All these truly avirulent strains were collected at t1 (Table S2). Five of the strains yielding dubious results that

induced pycnidia on CS-*Stb16q* were unable to infect Cellule, probably due to another source of resistance not present in CS. Similarly, two strains that induced pycnidia on Cellule were unable to infect CS-*Stb16q*. All 47 strains induced pycnidia on CS, confirming their pathogenicity.

Virulent strains were significantly more aggressive on CS-*Stb16q* than on Cellule (Wilcoxon test, $p < 0.0001$; Figure S9). No significant difference in aggressiveness (neither in AG nor AGc; $p = 0.054$ and $p = 0.060$, respectively; Figure S8) was detected between the avirulent and virulent strains that were pathogenic on Apache (2886/3035).

3.3 | Impact of mixtures on the dynamics of the virulent subpopulation

At the whole-canopy scale, cultivar proportions modulated the decreases in the size of the virulent subpopulation and in the frequency of virulent strains relative to the pure stand of the cultivar carrying *Stb16q* (Cellule).

In 2018, the mean size of the virulent subpopulation ($\overline{n}_{t2,vir}$) was significantly higher in pure stands of Cellule than in pure stands on Apache. However, $\overline{n}_{t2,vir}$ was not significantly different in mixtures than in pure stands of Cellule or Apache (Figure 7a). $\overline{n}_{t2,vir}$ tended to increase with the proportion of Cellule (p_C). In 2019, the three
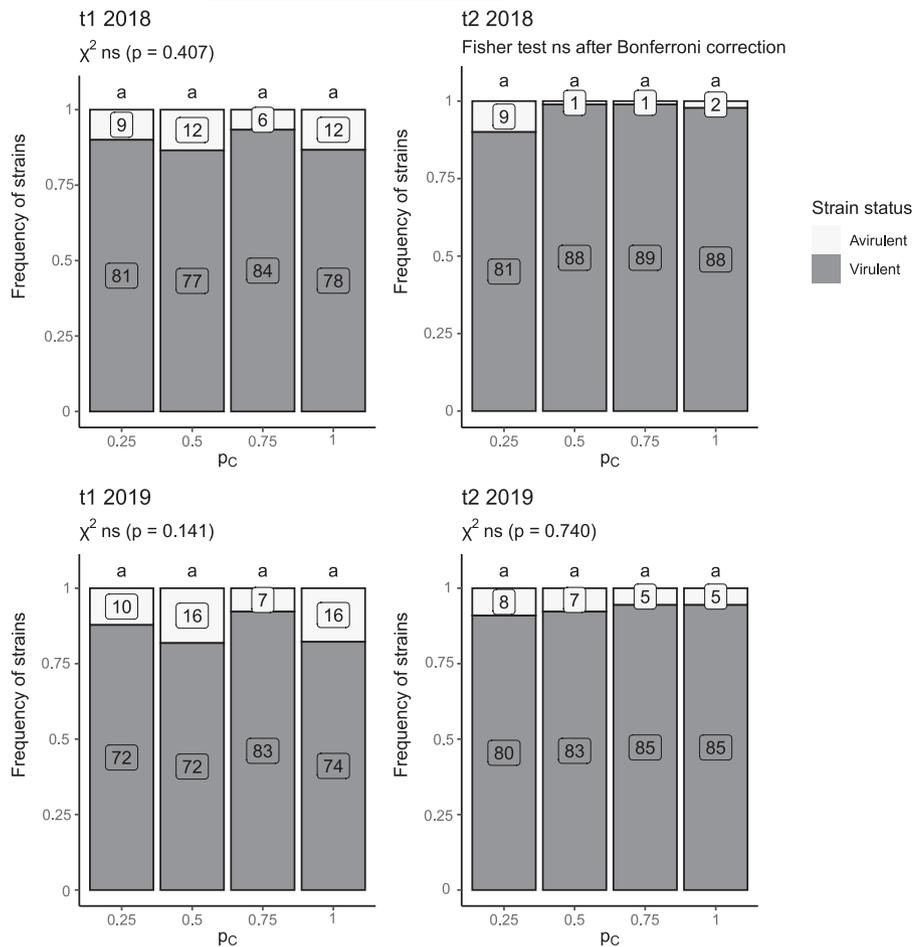
FIGURE 6 Frequency of *Zymoseptoria tritici* strains considered virulent (grey bars) against *Stb16q* (i.e., causing sporulating area on cv. Cellule) and avirulent (white bars) among the populations collected on cv. Cellule in pure stands ($p_C = 1$) and mixtures ($p_C = 0.25$, 0.5, and 0.75 for C1A3, C1A1, and C3A1, respectively) at the early (t1) and late (t2) stages of the 2018 and 2019 epidemics. The number of virulent and avirulent strains are indicated in grey and white boxes, respectively. The effect of treatment (pure stands and cultivar mixtures; letters at the top of each bar) on the number of virulent strains was assessed by performing a χ^2 test, or a Fisher's exact test when the expected numbers were small, with Bonferroni correction for pairwise comparison

mixtures significantly decreased $\overline{n}_{t2,vir}$ relative to the pure stand of Cellule (Figure 7b), whereas the difference was not significant relative to the pure stand of Apache. Figure 7b shows a correlation of means and variances, assuming that mixture may both reduce and stabilize the virulent subpopulation size compare to pure stands. In 2019, $\overline{n}_{t2,vir}$ in mixtures was lower than in the pure stand of Cellule by a factor of about 5 and lower than that in the pure stand of Apache by a factor of 2. This difference can be explained by the very low frequency of virulent strains on Apache ($f_{t2,A,vir}$) being compensated in 2018, and, to a greater extent in 2019, by the size of the pathogen population on Apache (SEV_A), resulting in a larger number of virulent strains ($\overline{n}_{t2,vir}$). A dissociated analysis of each varietal component of the mixture can provide insight on this point. On Apache, the size of the virulent subpopulation ($n_{t2,A,vir}$) was not significantly different between pure stands and mixtures in 2018 ($p = 0.200$, Kruskal–Wallis test; Figure S11a) or 2019 ($p = 0.578$, Kruskal–Wallis test; Figure S11c). On Cellule, the size of the virulent subpopulation ($n_{t2,C,vir}$) increased significantly with p_C in 2018 ($p = 0.033$) and 2019 ($p = 0.024$). Thus, only $n_{t2,C,vir}$ contributes to the differences at whole-canopy scale.

We examined the relationship between the indicators investigated. We first focused on the relationship between the overall disease severity ($\overline{SEV}$)—an indicator of the efficacy of the mixtures—and the overall size of the virulent subpopulation ($\overline{n}_{t2,vir}$), an indicator of *Stb16q* breakdown dynamics and, thus, a proxy for the impact

of the mixtures on resistance durability (Figure 7c,d). In both years, the overall trend was similar for the virulent subpopulation: $\overline{n}_{t2,vir}$ increased with the proportion of Cellule (p_C) whereas $\overline{SEV}$ decreased. In 2018, two mixtures (C1A1 and C3A1) displayed decreases for both $\overline{n}_{t2,vir}$ and $\overline{SEV}$ relative to the pure stands of Cellule and Apache. In the C1A3 mixture, $\overline{SEV}$ was slightly higher with a lower level of $\overline{n}_{t2,vir}$ than in other mixtures. The impact of mixtures was greater in 2019, with all mixtures decreasing both $\overline{n}_{t2,vir}$ and $\overline{SEV}$, which was, on average, lower than in pure stands of Apache by a factor of 10 and lower than that in pure stands of Cellule by a factor of 5. We then focused on the relationship between the mean frequency of virulent strains ($\overline{f}_{t2,vir}$) and the overall size of the virulent subpopulation ($\overline{n}_{t2,vir}$) (Figure 7e,f). Both years, $\overline{f}_{t2,vir}$ and $\overline{n}_{t2,vir}$ increased with p_C, whose quantitative impact was generally high for $\overline{f}_{t2,vir}$ but relatively limited for $\overline{n}_{t2,vir}$, especially in 2018 for mixtures (Figure 7e,f).

Finally, regardless of the indicator considered ($\overline{SEV}$, $\overline{n}_{t2,vir}$ or $\overline{f}_{t2,vir}$) and of relationship trends, the optimal p_C appeared to be about 0.5. However, our results suggest that moving away from this optimal proportion would have different effects on the three indicators.

4 | DISCUSSION

We found that pathogen population size, estimated on each cultivar but also at the whole-canopy scale, was smaller for mixtures than

FIGURE 7 Impact of mixtures on different indicators of the *Zymoseptoria tritici* virulent subpopulations and their relationships at whole-canopy scale. (a, b) Size of the virulent subpopulations at t2 ($\overline{n}_{t2,vir}$ dimensionless variable; black dots) according to the proportion of cv. Cellule (p_C) in 2018 and 2019. Grey dots indicate the mean value for each block and black dots the mean for each treatment. Bars represent the standard error within each block. Error propagation was taken into account. (c, d) Disease severity assessed at the whole-canopy scale at t2 ($\overline{SEV}$, determined as the percentage of the leaf area covered with pycnidia on flag leaves) according to the size of the virulent subpopulation ($\overline{n}_{t2,vir}$). (e, f) Frequency of virulent strains assessed at whole-canopy scale at t2 ($\overline{f}_{t2,vir}$) according to the size of the virulent subpopulations in 2018 and in 2019. Small dots indicate the mean value for each block, and large dots the mean value for each treatment. Different shades of blue represent the proportion of cv. Cellule (p_C)
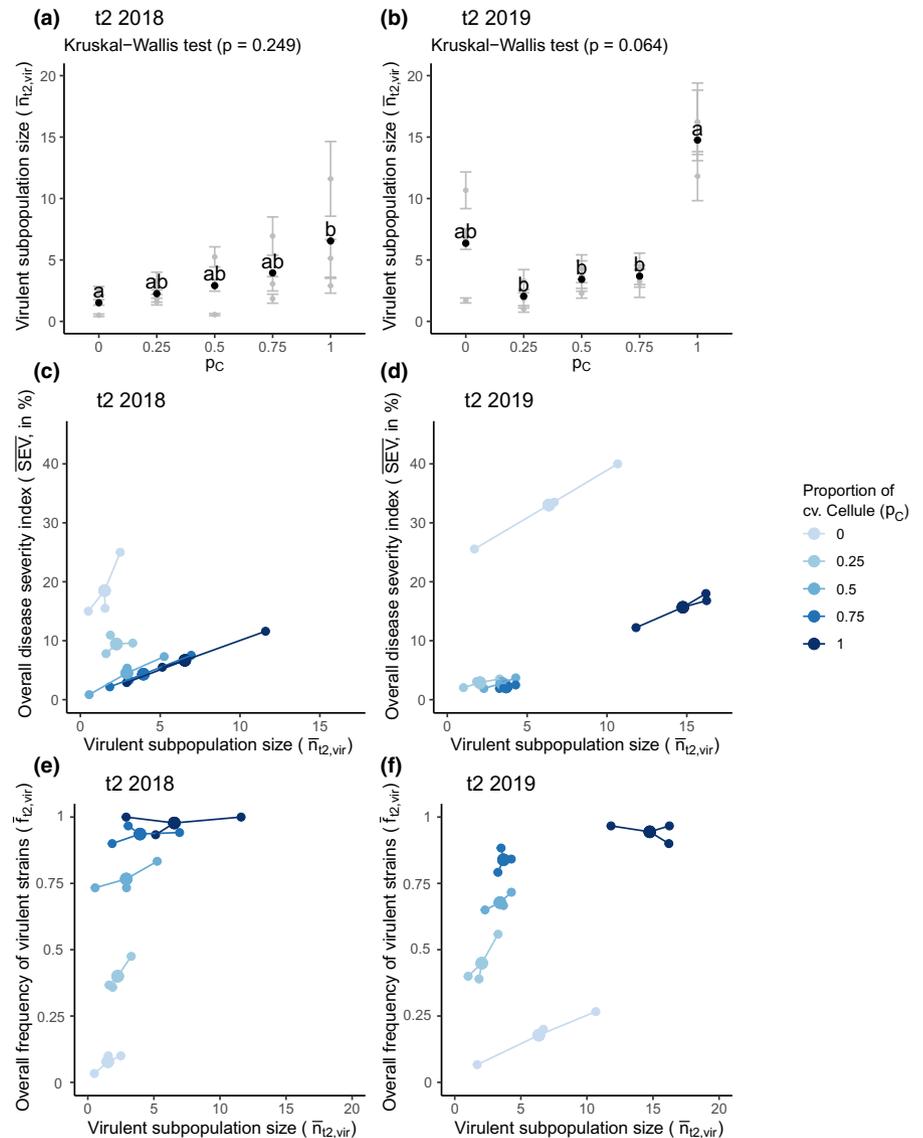
for pure stands at the end of epidemics. In addition we established that mixtures reduced the size of the virulent subpopulation by affecting the frequency of strains displaying virulence against *Stb16q*, relative to pure stands of Cellule (thereafter referred as the resistant cultivar).

Molecular tools are not always available for monitoring the emergence of virulence. This complicates the quantification of breakdown dynamics for recently deployed resistance genes. Our in planta population phenotyping, useful for this purpose, was twice as efficient as the classical method (Figure S3). The various experimental adjustments we made to inoculum preparation, climatic conditions in the greenhouse, visual assessments, and the small number of biological replicates (Table S3) introduced some uncertainty, potentially leading to diagnostic errors concerning virulence status at an individual scale ("false avirulence" rate estimated at 3%). However, this uncertainty had a small impact at the population scale.

We assumed that a strain pathogenic on cultivar Cellule was virulent against *Stb16q* and that a strain nonpathogenic on this cultivar was avirulent. However, as the genetic background of the Cellule

cultivar probably includes other sources of resistance, an absence of symptoms on Cellule is not sufficient to demonstrate avirulence against *Stb16q*. The confirmatory individual phenotyping data provide some perspective concerning this approximation: five of the seven strains inducing pycnidia on CS-*Stb16q* were unable to infect Cellule, and two of the strains pathogenic on Cellule were unable to develop sufficient pycnidia on CS-*Stb16q* to exceed the 10% threshold for virulence. The rarity of such situations (<1%) suggests that ability to induce pycnidia on Cellule is a reasonable indicator of virulence against *Stb16q*. Finally, we estimated that the virulence status established based on population phenotyping of the Cellule response was correct in 97% of cases.

Early in the epidemic, most of the time, the size of the pathogen population in the whole canopy ($\overline{SEV}$) and on both susceptible (SEV_A) and resistant (SEV_C) cultivars was not significantly different between mixtures and the corresponding pure stands (Figure 4). This is an expected result, as mixture effects were reported to increase during asexual cycles (Cowger & Mundt, 2002a; Gigot et al., 2013). Late in the epidemic, cultivar mixtures reduced $\overline{SEV}$,

confirming the potential of wheat mixtures to limit the dynamics of STB epidemics (Kristoffersen et al., 2019). In our experiment, mixtures reduced $\overline{SEV}$ by a mean of 27% in 2018 and 69% in 2019. The size of the pathogen population was lower in mixtures than in the corresponding pure stands only on the resistant cultivar in 2018 and on both cultivars in 2019. The relative differences in SEV_v between mixtures and pure stands ranged from 13% to 26% in 2018 and from 64% to 72% in 2019 for the susceptible cultivar, and from 19% to 69% in 2018 and from 70% to 80% in 2019 for the resistant cultivar. Gigot et al. (2013) and Vidal et al. (2017) highlighted similar reductions. The resistant cultivar acted as an obstacle to spore dispersal in mixtures and thus induced a barrier effect on the susceptible one (Wolfe, 1985). This protective effect has been reported before (Gigot et al., 2013) and was particularly strong in our study. Conversely, the presence of susceptible plants decreased the number of virulent strains filtered out by resistant plants relative to a pure stand of the resistant cultivar (Figure S11b,c). The susceptible plants did not concentrate more virulent strains in mixtures than in pure stands (Figure S11a,c), thereby decreasing the number of virulent strains at the whole-canopy scale. This may explain the protective effect of the susceptible cultivar on the resistant cultivar, which is a counterintuitive but crucial result.

We estimated the local frequency of virulent strains (0.13 in 2018 and 0.14 in 2019) using the pathogen population collected on pure stands of the susceptible cultivar early in the epidemic, which should reflect the founding ascospore population (Figure 1b). Some of the strains collected from sporulating lesions on Cellule early in the epidemic were avirulent. Two hypotheses may explain this: (a) the ontogeny or temperature-modulation of *Stb16q* expression in field conditions, and (b) the possibility of an avirulent strain coinfecting a host plant by taking advantage of infection with a virulent strain ("stowaway effect") or following systemic induced susceptibility (Seybold et al., 2020).

Mixtures modified the composition of the initial pathogen population by affecting strain selection during the epidemic. The frequency of virulent strains collected on the susceptible cultivar did not differ between pure stands and mixtures (Figure 5) early in the epidemic, when secondary infections were not yet strongly affecting disease dynamics. The differences expressed later, after several cycles of secondary infection, suggest that the mixture effect results from cross-contaminations between cultivars driven by pycnidiospore splash dispersal (Figure 1d), consistent with previous findings (Gigot et al., 2013; Vidal et al., 2017). In this study, the optimal proportion of the resistant cultivar minimizing the size of the virulent subpopulation ($\overline{n}_{t2,vir}$) and the frequency of virulent strains ($\overline{f}_{t2,vir}$) appeared to be about 0.25 (Figure 7e,f). The overall effect would probably be different for mixtures of cultivars with different combinations of resistance genes. For determining the consequences of multiple virulence–resistance interactions, a parallel could be drawn with studies focusing on the impact of wheat mixtures on the structure of yellow rust and powdery mildew populations (Lannou et al., 2005; Villaréal & Lannou, 2000) and on the emergence of multivirulent strains. It was shown that the frequency of such strains was not necessarily significantly higher in mixtures than in pure stands (Chin & Wolfe, 1984; Dileone & Mundt, 1994).

In theory, there should be a fitness penalty for pathogen populations with high levels of virulence after adaptation to hosts (Laine & Barrès, 2013). We did not find such a cost of virulence against *Stb16q* related to the aggressiveness trait that we studied (percentage of leaf area covered by pycnidia). This may be because the experimental conditions resulted in small mean sporulating areas (not entirely suitable for such a test), because this virulence has no cost—consistent with the experimental findings of Cowger and Mundt (2002b)—or because the cost concerns another aggressiveness trait (e.g., latent period, sporulation capacity of a pycnidia, infection efficacy; Suffert et al., 2013). Further studies, specially designed for this purpose, would help to progress on this issue.

We showed that changes in the overall size and composition of the pathogen population depended on the proportions of the two cultivars, consistent with previous findings (Finckh et al., 2000). All the mixtures efficiently decreased the size of the pathogen population ($\overline{SEV}$), but the decrease in severity relative to expected levels in the absence of a mixture effect (Figure 4) was greatest for C1A1 in both 2018 (40%) and 2019 (71%). In our experiment, the optimal proportion of the resistant cultivar for reducing $\overline{SEV}$ seemed to lie between 0.5 and 0.75. This is consistent with simulations performed by Gigot et al. (2014), which showed the protection of susceptible plants by resistant plants to be optimal for mixtures with more resistant than susceptible plants.

The intensity of epidemics, driven by climatic conditions, may account for the observed differences in the magnitude of the mixture effect. The epidemic started earlier in 2018 (Figure 4) and this year was wetter and cooler than 2019. However, STB severity ended up being more intense on flag leaves in 2019 (19% in 2018 vs. 33% in 2019 for SEV_A in C0A1; data not shown). This apparent contradiction can be explained by late spring rainfall at key moments for the epidemic, while the primary inoculum is rarely a limiting factor (Morais et al., 2016). Mixtures decreased the size of the total pathogen population more effectively in 2019. Mixtures also had a greater impact on the frequency of virulent strains on the susceptible cultivar relative to the pure stand (Figure 5) in 2018 than in 2019, whereas the opposite pattern might have been expected, due to more intense disease dynamics late in the epidemic (Mundt, 2002). Gigot et al. (2013) showed that mixtures significantly decreased disease severity in most cases, regardless of disease intensity, whereas Kristoffersen et al. (2019) found no correlation with mixture efficacy.

The choice of the indicator to analyse and the pure stand of reference is crucial. Our findings suggest that the optimal proportion of cultivars for reducing the size of the virulent subpopulation ($\overline{n}_{t2,vir}$) may differ slightly from that for reducing the size of the total pathogen population ($\overline{SEV}$), and that for reducing the overall frequency of virulent strains ($\overline{f}_{t2,vir}$) (Figure 7). The potential differences in the optima for these three indicators may conceal a trade-off between disease control and resistance durability. When comparing mixtures to the pure stands of the susceptible cultivar, disease severity can, indeed, be reduced by including a resistant cultivar in the host

population (Figure 4). However, this effect may be counterbalanced by an acceleration of the breakdown dynamics of this resistance, due to an increase in the frequency of virulent strains in susceptible plants. The conclusion would clearly be different if a pure stand of the resistant cultivar is used as the reference: the inclusion of susceptible plants decreased the selection pressure exerted by emerging virulent strains, but also, as shown here, decreased disease severity on the resistant plants. The pathogen population on the susceptible plants of a cultivar mixture may be smaller than that in a pure stand or in a mixture with a high proportion of the susceptible cultivar, without there necessarily being an impact on the number of virulent strains (Figure S11). From this perspective, mixtures appeared to slow down the breakdown dynamics of the resistance. Moreover, we did not find a trade-off between the size of the virulent subpopulation and the frequency of virulent strains, but there is no reason why this trend should be the same in other contexts. The "size" versus "frequency" debate is a classical issue in ecology that should not be neglected here, with consequences for genetic diversity and evolution (Brown & Tellier, 2011). Further studies are needed to determine if these dynamics would be different depending on the local frequency of virulent strains, that is, the breakdown stage of the resistance.

Determination of the effects of mixtures on the durability of the resistances deployed requires a consideration of the complete disease cycle, including sexual reproduction, and an extension of this approach to time scales beyond a single annual epidemic. One of the major issues arising from this study and previous studies (e.g., Finckh et al., 2000; Lannou et al., 2005; Mundt, 2002) is whether a cropping system based on cultivar mixtures would be likely to increase the prevalence of virulent strains after several years. This is both a question of the reference used (pure stand of a susceptible or resistant cultivar) and of the objective assigned to the mixture: decreasing disease severity relative to the pure stand of susceptible plants or increasing the durability of resistance by reducing the pressure exerted on the virulent subpopulation of the pathogen. Investigations of the longer term effects of cultivar mixtures need to consider sexual reproduction, as this process may either amplify or attenuate the demogenetic changes occurring during an annual epidemic. This is all the more relevant because a trade-off between size of pathogen population and frequency of virulence would impact the efficacy and durability, respectively, of the cultivar deployment strategies.

Recent landscape-scale models have investigated the effect of the proportion of fields sown with resistant and susceptible cultivars and their connectivity on the dynamics of resistance breakdown after several generations (e.g., Fabre et al., 2015). In comparisons of different strategies for preventing or delaying the appearance of a "superpathogen", cultivar mixtures appeared to be effective in the long term for pathogens with high mutation rates and high fitness costs (Crété et al., 2020; Rimbaud et al., 2018). Our experimental findings confirm that cultivar mixtures may also be used to extend the lifetime of resistance sources, this time at within-field scale, through the introduction of heterogeneity.

CONFLICT OF INTEREST

The authors declare that the research was conducted in the absence of any commercial or financial relationships that could be construed as a potential conflict of interest.

DATA AVAILABILITY STATEMENT

The data and the R scripts that support the findings of this study (Files F1–21, see list below) are freely available from the INRAE Dataverse online data repository (https://data.inrae.fr/) at https://doi.org/10.15454/4MAAI0. **File F1** (*F1_Field_disease_severity_raw-data.csv*). Field disease severity raw data. **File F2** (*F2_t2_2018_field-severity_means.txt*). Disease severity means per block, treatment, and cultivar used to calculate a proxy for the size of the virulent subpopulations. Data for the late stage of 2018 epidemic. **File F3** (*F3_t2_2019_field-severity_means.txt*). Disease severity means per block, treatment, and cultivar used to calculate a proxy for the size of the virulent subpopulations. Data for the late stage of 2019 epidemic. **File F4** (*F4_List_of_isolates.xls*). List and virulence status of the 3035 isolates phenotyped in the greenhouse. **File F5** (*F5_Disease_score_population-phenotyping_rawdata.xls*). Disease score raw data for the population phenotyping. **File F6** (*F6_t2_2018_population-phenotyping_virulents_number_R_on_R.txt*). Contingency table with the number of virulent and avirulent isolates per block and treatment, collected on Cellule and tested on Cellule, characterized with the population phenotyping. Data for the late stage of 2018 epidemic. **File F7** (*F7_t2_2018_population-phenotyping_virulents_number_R_on_S.txt*). Contingency table with the number of pathogenic and nonpathogenic isolates per block and treatment, collected on Cellule and tested on Apache, characterized with the population phenotyping. Data for the late stage of 2018 epidemic. **File F8** (*F8_t2_2018_population-phenotyping_virulents_number_S_on_R.txt*). Contingency table with the number of virulent and avirulent isolates per block and treatment, collected

on Apache and tested on Cellule, characterized with the population phenotyping. Data for the late stage of 2018 epidemic. **File F9** (*F9_t2_2018_population-phenotyping_virulents_number_S_on_S.txt*). Contingency table with the number of pathogenic and nonpathogenic isolates per block and treatment, collected on Apache and tested on Apache, characterized with the population phenotyping. Data for the late stage of 2018 epidemic. **File F10** (*F10_t2_2018_TabContglobal_virulence.txt*). Global contingency table with the number of virulent, avirulent, pathogenic, and nonpathogenic isolates per block, treatment, and cultivar collected in the field at the late stage of 2018 epidemic and tested with the population phenotyping. Data is used to calculate a proxy for the size of the virulent subpopulations. **File F11** (*F11_t2_2019_population-phenotyping_virulents_number_R_on_R.txt*). Contingency table with the number of virulent and avirulent isolates per block and treatment, collected on Cellule and tested on Cellule, characterized with the population phenotyping. Data for the late stage of 2019 epidemic. **File F12** (*F12_t2_2019_population-phenotyping_virulents_number_R_on_S.txt*). Contingency table with the number of pathogenic and nonpathogenic isolates per block and treatment, collected on Cellule and tested on Apache, characterized with the population phenotyping. Data for the late stage of 2019 epidemic. **File F13** (*F13_t2_2019_population-phenotyping_virulents_number_S_on_R.txt*). Contingency table with the number of virulent and avirulent isolates per block and treatment, collected on Apache and tested on Cellule, characterized with the population phenotyping. Data for the late stage of 2019 epidemic. **File F14** (*F14_t2_2019_population-phenotyping_virulents_number_S_on_S.txt*). Contingency table with the number of pathogenic and nonpathogenic isolates per block and treatment, collected on Apache and tested on Apache, characterized with the population phenotyping. Data for the late stage of 2019 epidemic. **File F15** (*F15_t2_2019_TabContglobal_virulence.txt*). Global contingency table with the number of virulent, avirulent, pathogenic, and nonpathogenic isolates per block, treatment, and cultivar collected in the field at the late stage of 2019 epidemic and tested with the population phenotyping. Data is used to calculate a proxy for the size of the virulent subpopulations. **File F16** (*F16_Severity_analysis.R*). Main script for field data analysis. **File F17** (*F17_Severity_function.R*). Function used in main script for field data analysis. **File F18** (*F18_Virulence_analysis.R*). Main script for population phenotyping data analysis. **File F19** (*F19_Virulence_function.R*). Function used in main script for population phenotyping data analysis. **File F20** (*F20_Realpop_analysis.R*). Main script to calculate the proxy for the size of the virulent subpopulations. **File F21** (*F21_Realpop_function.R*). Function used in main script to calculate the proxy for the size of the virulent subpopulations.

ORCID

Carolina Orellana-Torrejon 🄳 https://orcid.org/0000-0002-8108-8061

Tiphaine Vidal 🄳 https://orcid.org/0000-0001-8273-3205

Sébastien Saint-Jean 🄳 https://orcid.org/0000-0002-0401-0711

Frédéric Suffert 🄳 https://orcid.org/0000-0001-6969-3878

REFERENCES

Borg, J., Kiær, L.P., Lecarpentier, C., Goldringer, I., Gauffreteau, A., Saint-Jean, S. et al. (2018) Unfolding the potential of wheat cultivar mixtures: a meta-analysis perspective and identification of knowledge gaps. *Field Crops Research*, 221, 298–313.

Brown, J.K.M., Chartrain, L., Lasserre-Zuber, P. & Saintenac, C. (2015) Genetics of resistance to *Zymoseptoria tritici* and applications to wheat breeding. *Fungal Genetics and Biology*, 79, 33–41.

Brown, J.K.M. & Tellier, A. (2011) Plant–parasite coevolution: bridging the gap between genetics and ecology. *Annual Review of Phytopathology*, 29, 345–367.

Chartrain, L., Brading, P.A. & Brown, J.K.M. (2005) Presence of the *Stb6* gene for resistance to septoria tritici blotch (*Mycosphaerella graminicola*) in cultivars used in wheat-breeding programmes worldwide. *Plant Pathology*, 54, 134–143.

Chin, K. & Wolfe, M. (1984) Selection on *Erysiphe graminis* in pure and mixed stands of barley. *Plant Pathology*, 33, 535–545.

Cowger, C., Hoffer, M.E. & Mundt, C.C. (2000) Specific adaptation by *Mycosphaerella graminicola* to a resistant wheat cultivar. *Plant Pathology*, 49, 445–451.

Cowger, C. & Mundt, C.C. (2002a) Effects of wheat cultivar mixtures on epidemic progression of Septoria tritici blotch and pathogenicity of *Mycosphaerella graminicola*. *Phytopathology*, 92, 617–623.

Cowger, C. & Mundt, C.C. (2002b) Aggressiveness of *Mycosphaerella graminicola* isolates from susceptible and partially resistant wheat cultivars. *Phytopathology*, 92, 624–630.

Crété, R., Pires, R.N., Barbetti, M.J. & Renton, M. (2020) Rotating and stacking genes can improve crop resistance durability while potentially selecting highly virulent pathogen strains. *Scientific Reports*, 10, 19752.

Dileone, J. & Mundt, C. (1994) Effect of wheat cultivar mixtures on populations of *Puccinia striiformis* races. *Plant Pathology*, 43, 917–930.

Fabre, F., Rousseau, E., Mailleret, L. & Moury, B. (2015) Epidemiological and evolutionary management of plant resistance: optimizing the deployment of cultivar mixtures in time and space in agricultural landscapes. *Evolutionary Applications*, 8, 919–932.

Finckh, M., Gacek, E., Goyeau, H., Lannou, C., Merz, U., Mundt, C. et al. (2000) Cereal variety and species mixtures in practice, with emphasis on disease resistance. *Agronomie*, 20, 813–837.

Fones, H. & Gurr, S. (2015) The impact of Septoria tritici blotch disease on wheat: an EU perspective. *Fungal Genetics and Biology*, 79, 3–7.

Gigot, C., de Vallavieille-Pope, C., Huber, L. & Saint-Jean, S. (2014) Using virtual 3-D plant architecture to assess fungal pathogen splash dispersal in heterogeneous canopies: a case study with cultivar mixtures and a non-specialized disease causal agent. *Annals of Botany*, 114, 863–876.

Gigot, C., Saint-Jean, S., Huber, L., Maumené, C., Leconte, M., Kerhornou, B. et al. (2013) Protective effects of a wheat cultivar mixture against splash-dispersed Septoria tritici blotch epidemics. *Plant Pathology*, 62, 1011–1019.

Johnson, R. (1984) A critical analysis of durable resistance. *Annual Review of Phytopathology*, 22, 309–330.

Kildea, S., Byrne, J.J., Cucak, M. & Hutton, F. (2020) First report of virulence to the Septoria tritici blotch resistance gene *Stb16q* in the Irish *Zymoseptoria tritici* population. *New Disease Reports*, 41, 13.

Kristoffersen, R., Jørgensen, L.N., Eriksen, L.B., Nielsen, G.C. & Kiær, L.P. (2019) Control of Septoria tritici blotch by winter wheat cultivar mixtures: meta-analysis of 19 years of cultivar trials. *bioRxiv*, 658575.

Laine, A.-L. & Barrès, B. (2013) Epidemiological and evolutionary consequences of life-history trade-offs in pathogens. *Plant Pathology*, 62, 96–105.

Lannou, C. (2012) Variation and selection of quantitative traits in plant pathogens. *Phytopathology*, 50, 319–338.

Lannou, C., Hubert, P. & Gimeno, C. (2005) Competition and interactions among stripe rust pathotypes in wheat-cultivar mixtures. *Plant Pathology*, 54, 699–712.

McDonald, B.A. & Linde, C. (2002) Pathogen population genetics, evolutionary potential, and durable resistance. *Annual Review of Phytopathology*, 40, 349–379.

McIntosh, R.A. & Brown, G.N. (1997) Anticipatory breeding for resistance to rust diseases in wheat. *Annual Review of Phytopathology*, 35, 311–326.

McRoberts, N., Hughes, G. & Madden, L.V. (2003) The theoretical basis and practical application of relationships between different disease intensity measurements in plants. *Annals of Applied Biology*, 142, 191–211.

Morais, D., Sache, I., Suffert, F. & Laval, V. (2016) Is the onset of Septoria tritici blotch epidemics related to the local pool of ascospores? *Plant Pathology*, 65, 250–260.

Mundt, C.C. (2002) Use of multiline cultivars and cultivar mixtures for disease management. *Annual Review of Phytopathology*, 40, 381–410.

Niks, R.E., Parlevliet, J.E., Lindhout, P. & Bai, Y. (2011) *Breeding crops with resistance to diseases and pests*. Wageningen: Wageningen Academic Publishers.

Perronne, R., Makowski, D., Goffaux, R., Montalent, P. & Goldringer, I. (2017) Temporal evolution of varietal, spatial and genetic diversity of bread wheat between 1980 and 2006 strongly depends upon agricultural regions in France. *Agriculture, Ecosystems & Environment*, 236, 12–20.

Rimbaud, L., Papaix, J., Barrett, L.G., Burdon, J.J. & Thrall, P.H. (2018) Mosaics, mixtures, rotations or pyramiding: what is the optimal strategy to deploy major gene resistance? *Evolutionary Applications*, 11, 1791–1810.

Seybold, H., Demetrowitsch, T.J., Hassani, M.A., Szymczak, S., Reim, E., Haueisen, J. et al. (2020) A fungal pathogen induces systemic susceptibility and systemic shifts in wheat metabolome and microbiome composition. *Nature Communications*, 11, 1910

Suffert, F., Delestre, G. & Gélisse, S. (2018) Sexual reproduction in the fungal foliar pathogen *Zymoseptoria tritici* is driven by antagonistic density dependence mechanisms. *Microbial Ecology*, 77, 110–123.

Suffert, F., Sache, I. & Lannou, C. (2011) Early stages of Septoria tritici blotch epidemics of winter wheat: build-up, overseasoning, and release of primary inoculum. *Plant Pathology*, 60, 166–177.

Suffert, F., Sache, I. & Lannou, C. (2013) Assessment of quantitative traits of aggressiveness in *Mycosphaerella graminicola* on adult wheat plants. *Plant Pathology*, 62, 1330–1341.

Tabib Ghaffary, S.M., Faris, J.D., Friesen, T.L., Visser, R.G.F., van der Lee, T.A.J., Robert, O. et al. (2012) New broad-spectrum resistance to Septoria tritici blotch derived from synthetic hexaploid wheat. *Theoretical and Applied Genetics*, 124, 125–142.

Vidal, T., Boixel, A.-L., Durand, B., de Vallavieille-Pope, C., Huber, L. & Saint-Jean, S. (2017) Reduction of fungal disease spread in cultivar mixtures: impact of canopy architecture on rain-splash dispersal and on crop microclimate. *Agricultural and Forest Meteorology*, 246, 154–161.

Villaréal, L.M.M.A. & Lannou, C. (2000) Selection for increased spore efficacy by host genetic background in a wheat powdery mildew population. *Phytopathology*, 90, 1300–1306.

Wolfe, M.S. (1985) The current status and prospects of multiline cultivars and variety mixtures for disease resistance. *Annual Review of Phytopathology*, 23, 251–273.

SUPPORTING INFORMATION

Additional Supporting Information may be found online in the Supporting Information section.